Ultrastructure and Cytochemistry of Pectin and Cellulose Degradation in Tobacco Roots Infected by *Phytophthora parasitica* var. *nicotianae*

Nicole Benhamou and François Côté

Département de phytologie, Faculté des sciences de l'agriculture et de l'alimentation, Université Laval, Sainte-Foy, Québec, Canada, G1K 7P4. Correspondence and requests for reprints should be addressed to the first author. Present address of second author: Complex Carbohydrate Research Center, The University of Georgia, Athens, GA 30602.

Supported by the Natural Sciences and Engineering Research Council of Canada and by the Fonds pour la formation de chercheurs et l'aide à la recherche du Québec (FCAR). We thank Sylvain Noël for excellent technical assistance and M. T. Esquerré-Tugayé, Université Paul Sabatier, Toulouse, France, for providing the strain of *Phytophthora parasitica* var. *nicotianae*.

Accepted for publication 12 November 1991.

ABSTRACT

Benhamou, N., and Côté, F. 1992. Ultrastructure and cytochemistry of pectin and cellulose degradation in tobacco roots infected by *Phytophthora parasitica* var. *nicotianae*. Phytopathology 82:468-478.

Root colonization of tobacco (*Nicotiana tabacum* L. 'Xanthi-nc') by the pathogen *Phytophthora parasitica* var. *nicotianae* was studied by electron microscopy. Gold-complexed probes were used for the localization of pectin and cellulose. The epidermis was colonized from 24 to 48 h after inoculation, and the cortex appeared entirely colonized by the time the pathogen reached the paratracheal parenchyma (96 h after inoculation). The fungus did not penetrate the xylem vessels. Colonization of the root tissues was associated with changes, including alteration of primary cell walls and breakdown of middle lamella matrices. The pattern of pectin distribution, as revealed by the *Aplysia* gonad lectin-gold complex, indicated that the fungus produced pectic enzymes that diffused extracellularly. The release of pectic fragments and the accumulation of pectin molecules at specific sites such as the intercellular spaces were frequently detected. Cellulose was localized with an exoglucanase-gold complex, which showed that the fungus could produce cellulases but to a lesser extent than pectinases. Various host reactions were observed during pathogen ingress into the root; these reactions included the filling of intercellular spaces with a pectin-rich fibrillar material, the plugging of sieve pores and plasmodesmata with an amorphous material, and the occlusion of noninvaded xylem vessels by a coating material. Although highly susceptible to *P. p. nicotianae*, *N. tabacum* 'Xanthi-nc' appears capable of using a complex array of defense reactions. The possibility of sensitizing this cultivar to respond more rapidly to pathogen attack is raised.

Additional keywords: fungal colonization, gold labeling, host reactions.

The development of the tobacco black shank pathogen, *Phytophthora parasitica* var. *nicotianae* Tucker, on different cultivars of tobacco (*Nicotiana tabacum* L.) has received considerable attention in relation to disease incidence (18) and epidemiology (13,20). Cultural and biological control strategies have been suggested (19,26), but control is currently achieved through the use of cultivars that possess dominant genes for resistance to fungal attack (16,30). However, none of the cultivated tobacco genotypes has effective resistance to all races of the pathogen (30). Tobacco lines derived from *N. plumbaginifolia* and *N. longiflora* exhibited a high resistance to race 0 of *P. p. nicotianae* but were highly susceptible to race 1 (23).

Molecular mechanisms involved in the defense response of tobacco plants to *P. p. nicotianae* attack have been the focus of intensive research in recent years. The discovery that not only phytoalexins (12), proteinase inhibitors (34), and pathogenesis-related (PR) proteins (32) accumulate in fungus-infected tobacco plants to an extent similar to that in tobacco mosaic virus (TMV) inoculated plants has led to the consideration that expression of resistance is a nonspecific response of the host to pathogens (32). However, substantial evidence from several studies supports the concept that the ability of a plant to resist pathogens is related not only to the capability of activating the expression of defense genes, but it is also largely dependent on the coordination, speed, and magnitude with which the different defense strategies are expressed (29). The recent advances in molecular biology and plant transformation have provided a new basis for sensitizing plants to respond more rapidly to pathogens (27,35). Increased resistance to several fungi, including *Rhizoctonia solani* and *Botrytis cinerea* was recently reported to occur in transgenic tobacco plants that constitutively expressed a bean endochitinase gene (11). If the antifungal activity of chitinases is due to their hydrolytic activity on chitin, chitinase-transformed tobacco plants probably cannot afford resistance against fungi that, like *Phytophthora* spp., lack chitin in the cell walls. Manipulation of other gene expressions may enhance protection against this oomycete.

One alternative approach that has been reported to confer increased resistance to *P. p. nicotianae* is the enhancement of the natural hypersensitive response expressed by the host by a preinoculation with TMV or avirulent strains of the pathogen (10,31). Tobacco cultivars (i.e., Xanthi-nc) that react hypersensitively to TMV infection are protected against subsequent infections by *P. p. nicotianae* (10).

We are interested in understanding the molecular and cellular mechanisms involved in the relationship between induction of a hypersensitive response and protection against *P. p. nicotianae* in tobacco cv. Xanthi-nc. However, a prerequisite to this end is a thorough knowledge of the cytology of infection of tobacco plants by the pathogen. Determination of how induced defense mechanisms may restrict or inhibit pathogen growth obviously requires a detailed picture of the extent of fungal colonization and of host cell alterations during the normal infection process. To our knowledge, very little is known of the ultrastructural features of the interaction between susceptible tobacco cultivars and *P. p. nicotianae*. As a premise to further studies on induced protection by TMV inoculation, we report in the present study on the cytological changes that occur in *N. tabacum* 'Xanthi-nc' after infection with *P. p. nicotianae*. Particular attention has been placed on the patterns of pectin and cellulose degradation during pathogen ingress into the host.

MATERIALS AND METHODS

Fungal isolate and growth conditions. Race 0 of *P. p. nicotianae* (isolate 1156) was kindly provided by M. T. Esquerré-Tugayé

(Toulouse, France) who received it from J. P. Helgeson (Wisconsin). The fungus was grown on oatmeal agar as previously described (36) and maintained in the dark at 25 C. Zoospores were obtained 4–5 days later by chilling the plate (4 C for 30 min) and then returning it to room temperature (17). The concentration of zoospores was estimated with a hemacytometer and adjusted to 10^5 spores per milliliter by adding sterile distilled water.

Plant material and inoculation. The host plant used, *N. tabacum* 'Xanthi-nc', is hypersensitive to TMV and highly susceptible to *P. p. nicotianae*. Tobacco seeds were germinated in the greenhouse on vermiculite. Five-week-old seedlings were carefully removed from the vermiculite, and the roots were thoroughly washed with distilled water and inoculated by immersion for 1 h in distilled water that contained zoospores (10^5/ml). The plants were subsequently repotted in vermiculite. Root pieces were collected daily from 2 to 5 days after inoculation and processed for electron microscopy. Control plants were treated with distilled water. Experiments were repeated twice. For each experiment, 10 samples from five different inoculated roots and five noninoculated roots were collected.

Specimen processing for electron microscopy. Root samples were fixed in 3% (v/v) glutaraldehyde in 0.1 M sodium cacodylate buffer, pH 7.2, for 2 h at room temperature, dehydrated in an ethanol series, and embedded in Epon 812. Some samples were postfixed with 1% (w/v) osmium tetroxide in sodium cacodylate buffer for 1 h at 4 C before dehydration and embedding. Ultrathin sections were collected on formar-coated nickel grids. An average of three blocks per inoculated root per time after inoculation were sectioned. At each corresponding time interval, two blocks per noninoculated root were also sectioned. At least five serial sections from each block were examined under the electron microscope.

Preparation of the colloidal gold complexes. The exoglucanase, a β-1,4-D-glucan cellobiohydrolase (EC 3.2.1.21) purified in a five-step procedure from a cellulase produced by the fungus *Trichoderma harzianum* Rifai (4,5), was used for localizing cellulosic β-1,4-glucans. The *Aplysia* gonad lectin (AGL), a lectin isolated from the gonads of the sea mollusc *Aplysia depilans* (22), was used for localizing polygalacturonic acid containing molecules (6,7).

Colloidal gold with particles averaging 15 nm in diameter was prepared according to Frens (21). The exoglucanase was complexed to gold at pH 9.0 and the AGL at pH 9.5 (5,7). Both complexes were resuspended after centrifugation in 0.5 ml of phosphate-buffered saline (PBS) (pH 6.0 for the exoglucanase and pH 8.0 for the AGL) that contained 0.02% (w/v) polyethylene glycol (PEG) 20,000 and were stored at 4 C until used.

Cytochemical labeling. Ultrathin sections were first floated on a drop of PBS-PEG at the pH used for resuspension for 5 min, then transferred to a drop of the gold complex for 30 min at room temperature in a moist chamber. They were washed with PBS, pH 7.2, rinsed with distilled water, and stained with uranyl acetate and lead citrate.

Specificity of the labeling was assessed by the following control tests: incubation with the probe to which was previously added its corresponding substrate or sugar (β-1,4-glucans from barley for the exoglucanase and polygalacturonic acids from citrus for the AGL, 1 mg/ml in PBS, pH 7.2); incubation with the uncomplexed protein, followed by incubation with the gold complex; and incubation with the gold suspension alone.

Quantification of labeling. The density of labeling over cell walls was determined by counting the number of gold particles per square micrometers. Area determinations were carried out by the point counting method, according to Weibel (37), which used negatives of electron micrographs projected on a lattice. The amount of labeling over a specified wall area (*Sa*) was estimated by counting the number of gold particles (*Ni*) on a photographic enlargement. The density of labeling (*Ns*) was calculated as: $Ns = Ni/Sa$, in which *Ns* represents the number of gold particles per unit surface. Densities were determined by counting the number of gold particles over specified wall areas

TABLE 1. Density of labeling obtained with the gold-complexed *Aplysia* gonad lectin (AGL) over primary walls of infected tobacco root cells at various times after inoculation with *Phytophthora parasitica* var. *nicotianae*

Time after inoculation (h)	Primary walls[a]					
	Outermost wall layers	C.V.[b] (%)	Middle lamella	C.V. (%)	Innermost wall layers	C.V. (%)
Noninoculated tissues	108.2[a] ± 25.5[b]	24	155.5 ± 18.3	12	99.9 ± 31.1	31
48	98.7 ± 9.9	10	52.4 ± 10.8	21	76.2 ± 25.1	33
Inoculated tissues						
72	85.6 ± 9.1	11	35.5 ± 10.1	28	50.8 ± 31.8	63
96	84.5 ± 18.3	22	14.3 ± 8.2	57	45.4 ± 20.9	46
120	62.3 ± 42.5	68	8.2 ± 7.4	90	31.9 ± 15.2	48

[a] Densities were determined by counting the number of gold particles over specified wall areas on 20 micrographs from two serial sections per sample per time after inoculation. Three root samples from five inoculated and five noninoculated plants were examined. Density of labeling is expressed by the number of gold particles per μm^{-2} ± SD.
[b] Coefficient of variation.

TABLE 2. Density of labeling obtained with the gold-complexed *Aplysia* exoglucanase over primary walls of infected tobacco root cells at various times after inoculation with *Phytophthora parasitica* var. *nicotianae*

Time after inoculation (h)	Primary walls[a]					
	Outermost wall layers	C.V.[b] (%)	Middle lamella	C.V. (%)	Innermost wall layers	C.V. (%)
Noninoculated tissues	182.4[a] ± 8.3[b]	5	93.6 ± 13.2	14	158.8 ± 10.7	7
48	175.9 ± 12.2	7	84.1 ± 28.3	34	131.5 ± 13.1	10
Inoculated tissues						
72	169.7 ± 24.1	14	79.2 ± 33.4	42	87.3 ± 31.2	36
96	91.5 ± 38.9	43	75.4 ± 25.8	34	38.6 ± 25.4	66
120	54.3 ± 41.2	76	42.1 ± 18.9	45	11.9 ± 10.8	91

[a] Densities were determined by counting the number of gold particles over specified wall areas on 20 micrographs from two serial sections per sample per time after inoculation. Three root samples from five inoculated and five noninoculated plants were examined. Density of labeling is expressed by the number of gold particles per μm^{-2} ± SD.
[b] Coefficient of variation.

on 20 micrographs taken from at least two serial sections per block of noninoculated and inoculated tobacco roots per time after inoculation. Quantitative data were, thus, established from: five inoculated roots and five noninoculated roots; three samples from each root; and two serial sections from each sample. Quantification was determined for each of the two experiments performed in this study. Because results were highly similar from one experiment to another, only results from experiment 1 are presented in Tables 1 and 2.

Reagents. The exoglucanase was kindly provided by C. Breuil, Forintek, Canada, and the AGL was provided by N. Gilboa-Garber, Bar Ilan University, Israel. Tetrachloroauric acid was purchased from BDH Chemicals, Montreal, Quebec, Canada. All other reagents for electron microscopy were obtained from JBEM Chemical Co., Pointe-Claire, Québec, Canada.

RESULTS

Cytology of infection of tobacco root cells by *P. p. nicotianae*. At each time interval, approximately 10 sections from each of the five inoculated roots were examined. Penetration of the root epidermis was often seen by 24 h after inoculation. By this time, a large number of zoospores had encysted and germinated on the root surface and formed a dense mycelium. From 24 to 48 h after inoculation, root colonization was intense beneath the epidermis (Fig. 1A) and was seen occasionally in the first outer cortical cells. Fungal growth was mainly intracellular and was associated with apparent epidermal cell death as judged by the marked degradation of the cytoplasm (Fig. 1A). Cytoplasm breakdown was not limited to invaded cells but was frequently detected in advance of pathogen ingress and/or in cells near a

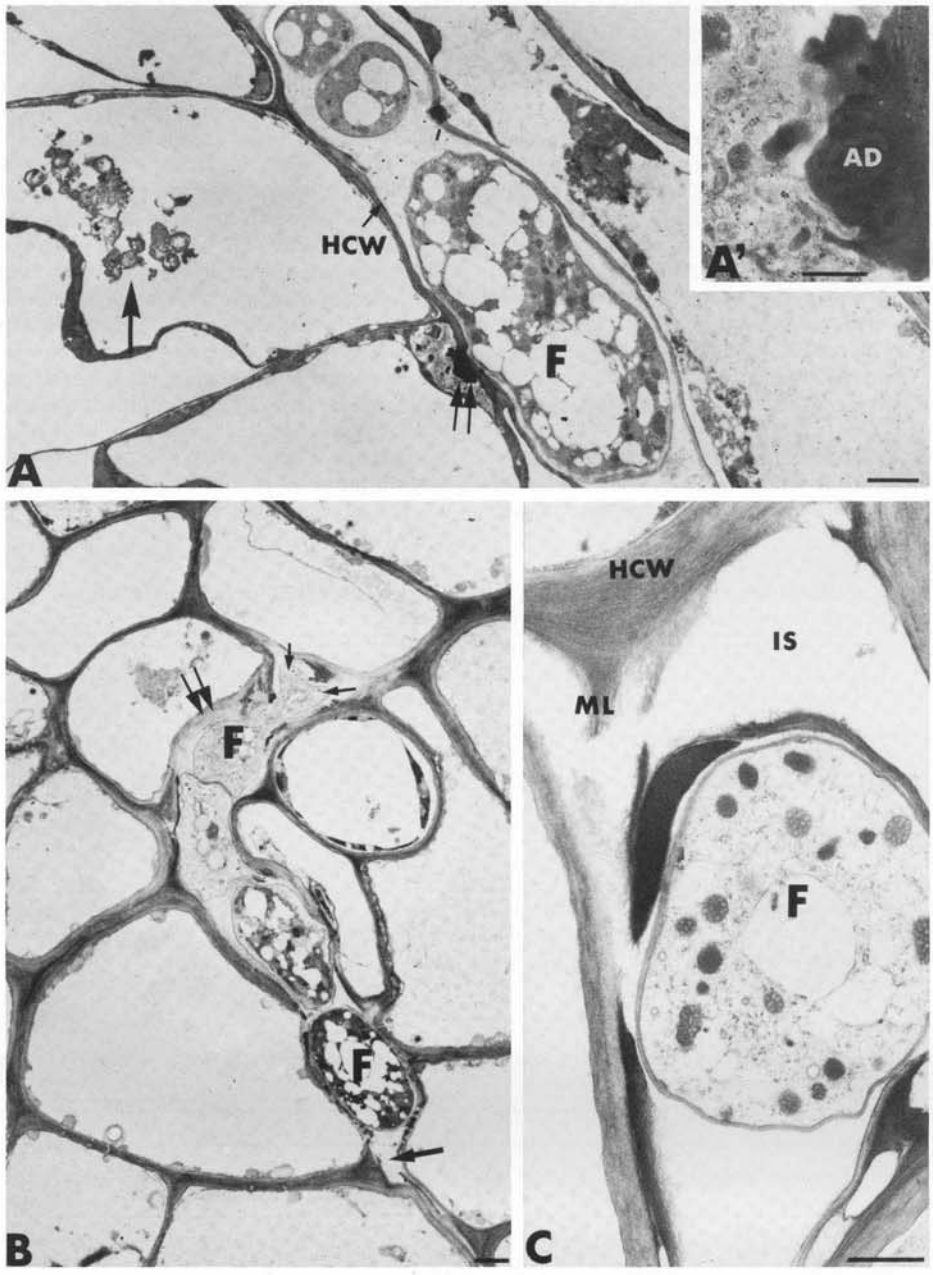

Fig. 1. Transmission electron micrographs of *Phytophthora parasitica* var. *nicotianae* infected tobacco root cells **A,** 48 h, or **B,C,** 72 h after inoculation. Samples were fixed with glutaraldehyde and osmium tetroxide. **A,** fungal growth in the epidermis is associated with marked host cytoplasm alteration (arrow). Electron-opaque amorphous deposits can be seen along a host wall area adjacent to an invading fungal cell (double arrows) (×9,000; bar: 1 μm). **A',** a portion of A at a higher magnification, which shows that the electron-opaque, amorphous deposit is surrounded by a material that contains vesiclelike structures (×21,500; bar: 0.5 μm). **B,** by 72 h after inoculation, the fungus develops abundantly in the cortex causing host wall alterations (double arrows). Disruption of the middle lamella matrix can be seen at a distance from the fungus (arrow). An invading hypha has branched (small arrows) (×4,500; bar: 1 μm). **C,** a fungal cell in an intercellular space. The middle lamella is highly altered (×27,000; bar: 0.5 μm). Abbreviations: AD, amorphous deposit; HCW, host cell wall; F, fungus cell; ML, middle lamella; IS, intercellular space.

colonized area (Fig. 1A, arrow). Examination of serial sections revealed that fungal growth in the epidermis was not associated with marked changes in the structure of host cell walls, because signs of swelling or disintegration were seldom observed (Fig. 1A). By contrast, amorphous, electron-opaque deposits resembling papillae frequently occurred along host wall areas in noninfected cells adjacent to invaded ones (Fig. 1A, double arrow; 1A'). The ultrastructure of *P. p. nicotianae* hyphae was essentially as reported by Hemmes (25) with a dense cytoplasm, numerous polymorphic vacuoles, and thin cell walls.

By 72 h after inoculation, the fungus had developed through much of the cortex and caused extensive cell alterations (Fig. 1B). Growth was mainly intercellular, although host wall penetration was sometimes observed. Hyphae in the invaded cortex were often branched (Fig. 1B, small arrows) and showed great variations in size and shape (Fig. 1B) as shown by serial sections. Pathogen ingress into the cortex was always associated with considerable host wall alterations, ranging from swelling and shredding (Fig. 1B, double arrows) to complete disruption of the middle lamellar matrices (Fig. 1C), which often occurred at a distance from the fungus (Fig. 1B, large arrow). Host cells near the colonized area showed pronounced disorganization characterized by plasmolysis and cytoplasm aggregation (Fig. 1B).

From 72 to 96 h after inoculation, an abrupt increase in the number of invading hyphae was inferred. Fungal cells multiplied abundantly and radiated rapidly into the endodermis, the pericycle, and the paratracheal parenchyma cells. Fungal growth occurred intercellularly, intracellularly, and intramurally (Fig.

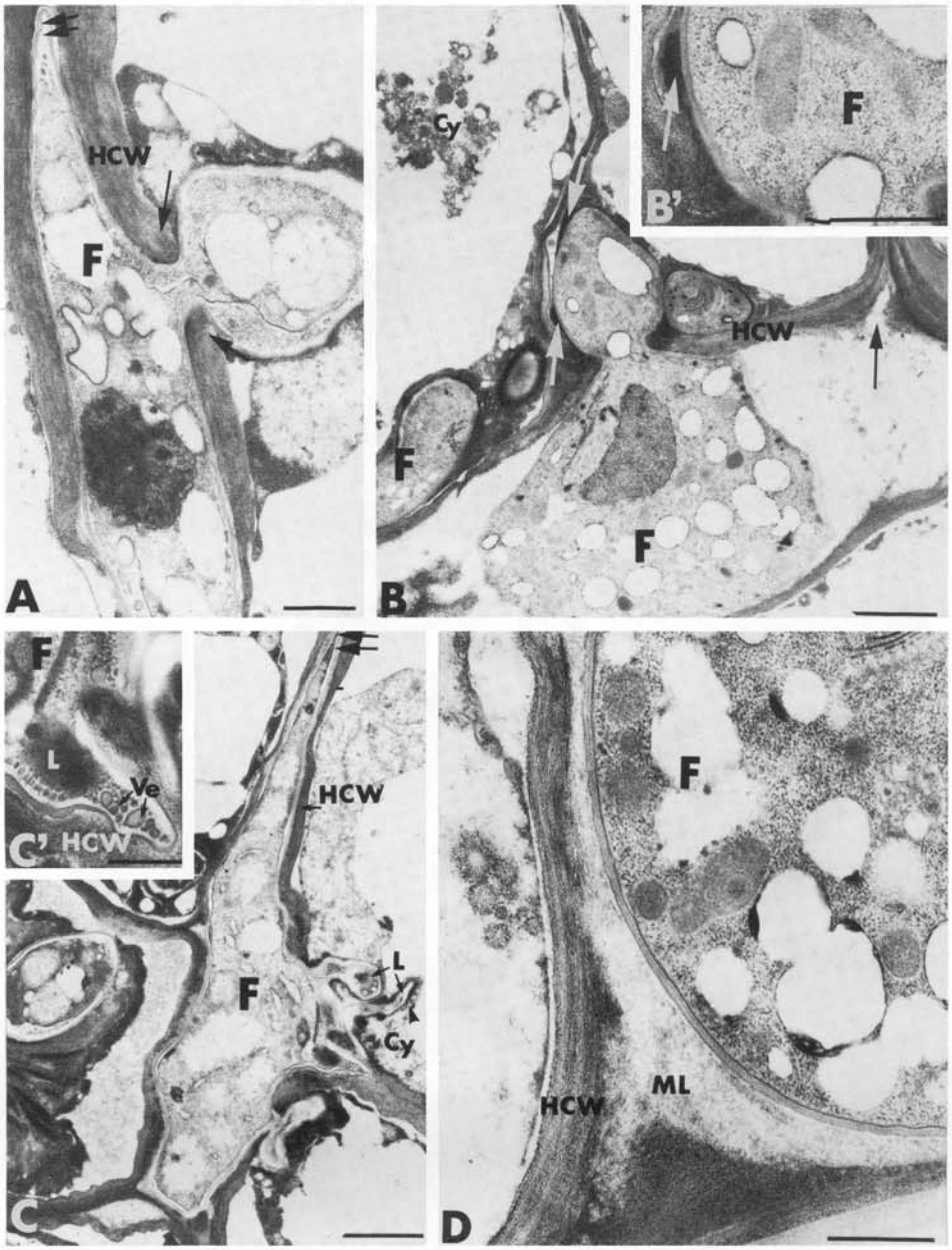

Fig. 2. Transmission electron micrographs of *Phytophthora parasitica* var. *nicotianae* infected tobacco root cells 96 h after inoculation. **A,** a host cell wall in the endodermis was penetrated by a fungal cell. The channel of penetration is much narrower than the average hyphal diameter. Little host wall displacement is observed in the direction of fungal growth (arrows). The fungal cell is more elongated than normal, with a very thin portion (double arrows) (×21,500; bar: 0.5 μm). **B,** alteration of the middle lamella is seen at a long distance from the point of fungal penetration (black arrow). Electron-opaque deposits are seen along the intracellular hyphal structure (white arrows) (×14,500; bar: 1 μm). **B',** a portion of B at a higher magnification, which shows the occurrence of an electron-opaque deposit along the fungus cell wall (white arrow) (×36,000; bar: 0.5 μm). **C,** a multilobed hypha growing intramurally. The lobes are polymorphic and contain numerous vesicles (×14,500; bar: 1 μm.). **C',** a portion of this hypha is much thinner than normal (double arrows) (×27,000; bar: 0.5 μm). **D,** fungal growth in the paratracheal parenchyma is associated with pronounced middle lamella alterations (×36,000; bar: 0.5 μm). Abbreviations: F, fungus cell; L, lobe; Ve, vesicle; HCW, host cell wall; Cy, cytoplasm; ML, middle lamella.

2A). Host cytoplasm in the invaded cells was markedly altered and often reduced to fine, electron-opaque strands in which organelles were no longer discernible (Fig. 2B,C). Pathogen ingress into these tissues was also associated with a considerable alteration of the host cell walls and middle lamella matrices even at a distance from the point of hyphal penetration (Fig. 2B, black arrow; 2D). Serial sections showed that host wall penetration was achieved by means of constricted hyphae (Fig. 2A,B); penetration channels were much narrower than the average hyphal diameter. Little host wall displacement in the direction of fungal growth was usually observed at sites of penetration (Fig. 2A, arrows). Interestingly, electron-opaque deposits were frequently seen along the haustoriumlike body (Fig. 2B,B', white arrows). When growing within host cell walls, hyphae exhibited considerable changes in morphology (Fig. 2A,C). These hyphae were usually more elongated than normal and had apparently very thin apical portions in wall areas between closely appressed adjacent host cells (Fig. 2A,C, double arrows). Another typical feature of such hyphae was the formation of polymorphic lobes that appeared as short, fingerlike projections into the adjacent host cell (Fig. 2C, arrowhead). Examination of these lobes at a high magnification revealed that conspicuous inclusion vesicles accumulated near the tip (Fig. 2C'). Such particular features were seen in all examined sections, thus indicating that it was not an artifact of section angle.

Colonization of the vascular area occurred between 96 and 120 h after inoculation and proceeded via the invasion of the paratracheal parenchyma cells (Fig. 3A). The massive colonization of these cells resulted in marked alterations, including cytoplasm disintegration, cell collapse (Fig. 3A, white arrow), and wall breakdown (Fig. 3A, double arrows). Branched hyphae grew mainly along the middle lamella, but some were intracellular,

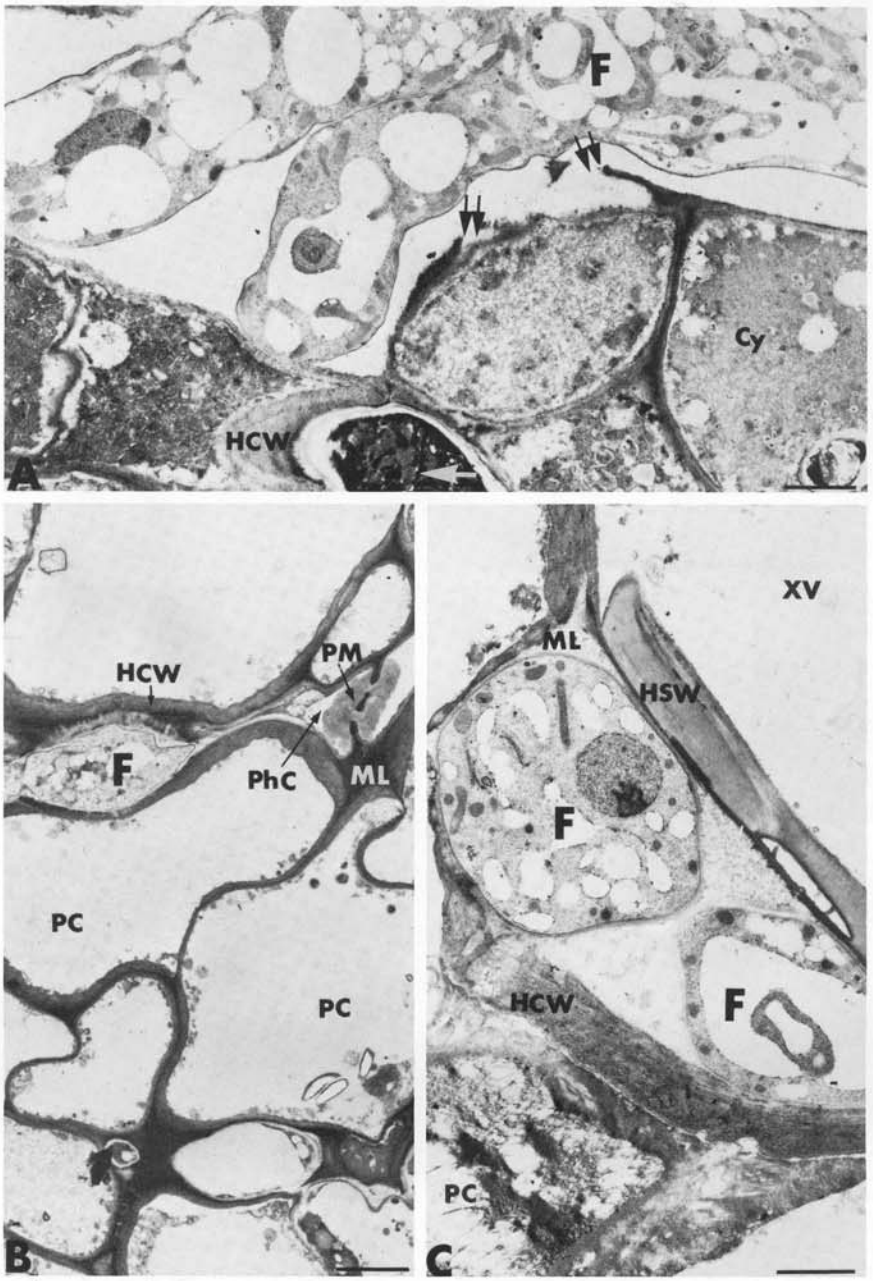

Fig. 3. Transmission electron micrographs of *Phytophthora parasitica* var. *nicotianae* infected tobacco root cells 120 h after inoculation. **A,** colonization of the paratracheal parenchyma is associated with cytoplasm disintegration, cell collapse (white arrow), and wall breakdown (double arrows) (×14,500; bar: 1 μm). **B,** a fungal cell was growing centripetally towards a phloem cell. The sieve pores in the phloem cell are completely plugged by large amounts of a plugging material (×12,000; bar: 1 μm). **C,** a paratracheal parenchyma cell adjacent to an uninvaded xylem vessel is markedly altered. The middle lamella matrix is disrupted, whereas the host secondary wall is apparently unaltered (×27,000; bar: 0.5 μm). Abbreviations: F, fungus cell; HCW, host cell wall; Cy, cytoplasm; PC, parenchyma cell; PhC, phloem cell; PM, plugging material; ML, middle lamella; HSW, host secondary wall.

invading the lumen of damaged cells. The pathogen grew centripetally directly through tangential walls towards the sieve elements (Fig. 3B). The main noticeable modification of noninvaded phloem cells adjacent to colonized parenchyma cells was the intense deposition of an amorphous material that completely plugged the sieve pores (Fig. 3B). Some phloem cells were entirely filled by this electron-opaque material. Successful penetration of the xylem vessels was seldom observed. This contrasted with the massive colonization of adjacent paratracheal parenchyma cells and the pronounced alteration of the middle lamella matrices (Fig. 3C). Various host reactions were observed within the noncolonized xylem vessels, such as the formation of a network of polymorphic bubblelike structures lining the secondary thickenings and coating the pit cavities (Fig. 4A). Another typical reaction was the coating of some vessels with a fine matrix of fibrillar material (Fig. 4B). A third type of reaction commonly observed was the complete plugging of the vessel lumen with an electron-dense, aggregated material of higher compactness and opacity that appeared along the secondary thickenings and pit cavities (Fig. 4C). Tyloses similar to those described in xylem vessels colonized by vascular wilt fungi were not observed. These reactions in the xylem vessels of infected roots were never seen in noninfected plants. At this time after inoculation (120 h), leaf chlorosis and incipient leaf flaccidity were usually observed on infected plants.

Cytochemical localization of pectic substances. The lectin from the gonads of *A. depilans* (AGL) (22), a polygalacturonic acid-binding agglutinin (6,8), was applied to infected tobacco root tissues for studying the pattern of pectin distribution in host cell walls. Cells of *P. p. nicotianae* grown in culture did not react with the gold-complexed lectin, as judged by the absence of labeling (Fig. 5A). As previously reported for other plants (6,8), labeling with the AGL-gold complex was associated with primary cell walls and middle lamella matrices in noninoculated tobacco root cells (not shown). Examination of infected tissues from 48 to 120 h after inoculation showed that labeling with the gold-complexed lectin was markedly reduced in wall areas exhibiting signs of obvious damage (Table 1; Fig. 5B). Intercellular growth of the pathogen was accompanied by considerable alteration of the middle lamella, which could be reduced to a network of lightly labeled fine fibrils (Fig. 5B). Development of the pathogen in the lumen of host cells was also associated with severe disruption (Fig. 5C). Incubation with the AGL-gold complex resulted in an irregular deposition of gold particles over host primary walls (Table 1; Fig. 5C). Labeling was, indeed, preferentially associated with the outermost wall layers (Fig. 5C, arrows), whereas only a few scattered gold particles occurred over the more internal wall layers, which appeared as a loosely arranged matrix of intertwined fibrils (Fig. 5C, double arrows). A large number of fibrillar fragments, likely detached from the altered innermost wall layers, were seen in the lumen of invaded host cells. These fragments were specifically labeled by gold particles (Fig. 5C, arrowheads).

During pathogen ingress towards the vascular stele, some host reactions occurred. One of the most noticeable reactions was the filling of some uninvaded intercellular spaces with a fibrillar matrix that specifically reacted with the gold-complexed AGL (Fig. 5D). Host walls surrounding invaded intercellular spaces were often thickened by a fibrillo-granular material, the structure of which appeared usually much less compact than that of the papillae described in vascular wilt infections (8). A close examination of this material showed that it was specifically labeled by the gold-complexed AGL (Fig. 5E,E'). Reactions in xylem vessels, such as bubblelike structures and coating material, were always free of labeling (not shown). As previously described with other infected plant tissues (6,8), specificity of the labeling obtained with the AGL-gold complex was assessed through the negative results generated by all control tests, including preincu-

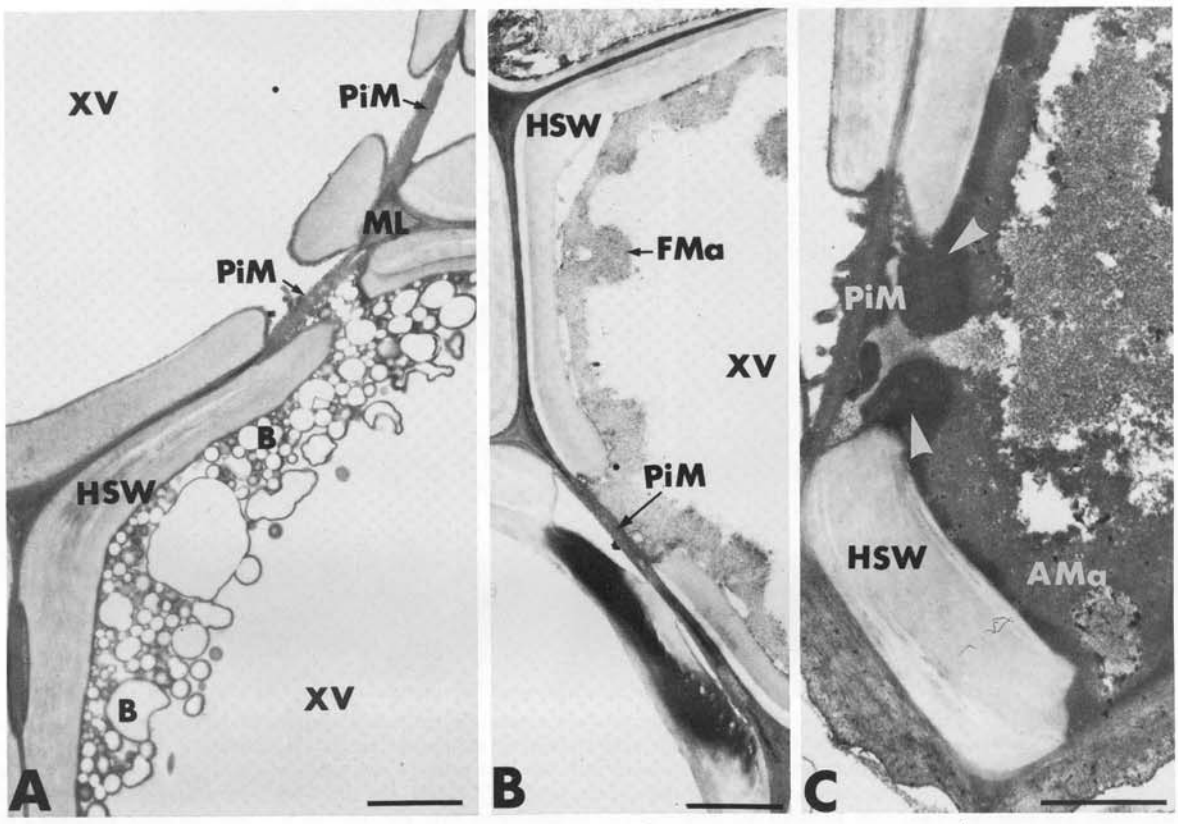

Fig. 4. Transmission electron micrographs of *Phytophthora parasitica* var. *nicotianae* infected tobacco root cells 96–120 h after inoculation. Various host reactions occurred within noninvaded xylem vessels during the infection process. These reactions include: **A,** the formation of bubblelike structures (×27,000; bar: 0.5 μm); **B,** the coating with a fine matrix of fibrillar material (×27,000; bar: 0.5 μm); or **C,** the complete plugging of the lumen by an electron-opaque, amorphous material (×36,000; bar: 0.5 μm). Abbreviations: XV, xylem vessel; PiM, pit membrane; ML, middle lamella; HSW, host secondary wall; B, bubble; FMa, fibrillar material; AMa, amorphous material.

bation of the complex with polygalacturonic acids before section labeling (not shown).

Cytochemical labeling of cellulose. Examination of ultrathin sections of *P. p. nicotianae* colonies incubated with the gold-complexed exoglucanase revealed the occurrence of an intense labeling over the fungus cell walls (Fig. 6A). In contrast, cytoplasm, vacuoles, and organelles were free of gold particles. Observation of a large number of sections indicated that gold labeling was predominantly associated with the more internal wall layers of *P. p. nicotianae* cells (Fig. 6A, arrow), whereas the outermost wall layers were nearly unlabeled (Fig. 6A, arrowhead).

Incubation of sections from noninoculated tobacco root tissue with the enzyme-gold complex resulted in a heavy labeling of primary (Table 2; Fig. 6B) and secondary cell walls. Cytoplasm and organelles were always unlabeled.

Between 48 and 72 h after inoculation, the fungus had colonized the epidermis and much of the cortex, causing extensive cell damage and wall alteration. Incubation of these infected tissues with the gold-complexed exoglucanase resulted in the deposition of gold particles over both fungal and plant cell walls (Fig. 6C,D). Labeling of the fungal walls was similar to that noted over the fungus grown in culture, although it appeared more evenly distributed throughout the entire wall (Fig. 6C). Great variations in labeling intensity were observed over host cell walls adjacent to invading hyphae (Table 2; Fig. 6D,E). Usually, labeling was not totally abolished even over markedly altered host cell walls

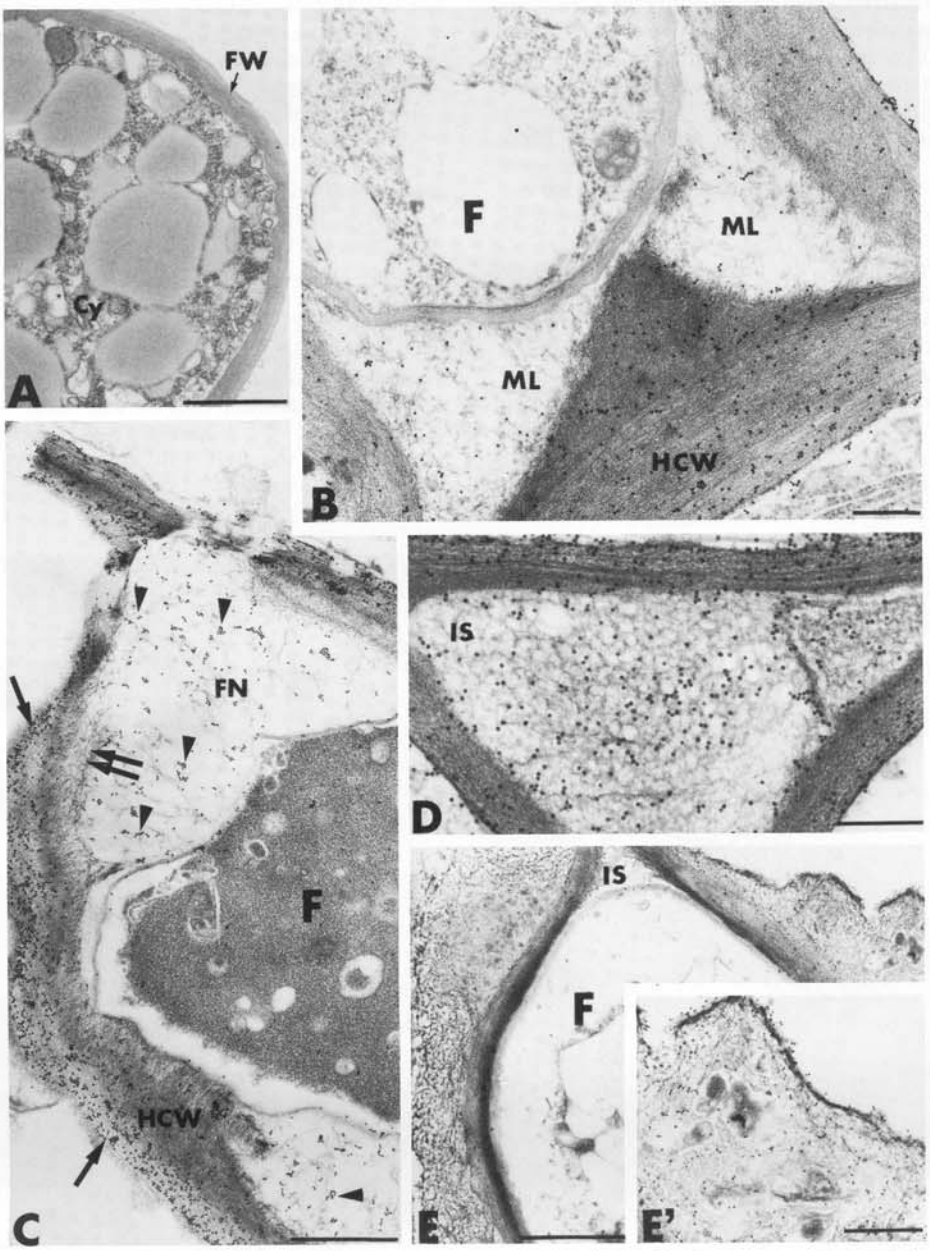

Fig. 5. Transmission electron micrographs of *Phytophthora parasitica* var. *nicotianae* infected tobacco root cells labeled with the gold-complexed *Aplysia* gonad lectin (AGL) for the localization of polygalacturonic acid containing molecules (pectin). **A,** labeling is absent over a fungal cell grown in culture (×36,000; bar: 0.5 μm). **B,** gold particles are associated with the host primary cell wall and the unaltered portion of the middle lamella. A very light labeling occurs over the damaged areas of the middle lamella (×45,000; bar: 0.25 μm). **C,** a fungal cell was growing in a host cortical cell. Over the host cell wall, gold particles are preferentially concentrated over the outermost layers (arrows), whereas a very light labeling occurs over the innermost, shredded layers (double arrows). Fibrillar fragments likely detached from the host cell wall are heavily labeled (arrowheads) (×36,000; bar: 0.5 μm). **D,** the fibrillar material filling an intercellular space is substantially labeled (×54,000; bar: 0.25 μm). **E,** a fibrillo-granular material accumulates along the walls of an invaded intercellular space (×18,000; bar: 1 μm); **E',** a portion of E at a higher magnification, which shows the occurrence of gold particles over this material (×27,000; bar: 0.5 μm). Abbreviations: FW, fungal wall; F, fungus cell; ML, middle lamella; HCW, host cell wall; FN, fibrillar network; IS, intercellular space.

characterized by pronounced swelling and shredding (Fig. 6E). The presence of a few scattered gold particles over the remaining fibrillar network indicated the preservation of some enzyme-binding sites, although occasionally labeling was found to be absent over wall portions that faced the invading hyphae (Fig. 6D, arrows). The fibrillar matrix that extended into the lumen of invaded host cells and around the pathogen was lightly labeled (Fig. 6E). Intramural growth of the fungus was accompanied by the alteration of some delineated wall areas (Fig. 7C, arrows) over which a considerable reduction of labeling occurred (Table 2). By contrast, heavy labeling still occurred over the apparently unaltered wall portions, although they were closely appressed against the fungus (Fig. 7C, double arrows).

The deposition of an electron-opaque, amorphous material along the wall of noninfected cells adjacent to colonized cells was often observed (Fig. 7A). This material, which plugged the plasmodesmata (Fig. 7A, arrowheads), was not labeled with the exoglucanase-gold complex (Fig. 7B). Among the other host reactions, only fibrillar wall thickenings similar to those illustrated in Figure 5E were labeled. The material that filled some intercellular spaces as well as the structures formed in xylem vessels were free of labeling (not shown). All control tests, including the previous adsorption of the enzyme-gold complex with β-1,4-glucans from barley, yielded negative results (Fig. 7D).

DISCUSSION

The present ultrastructural and cytochemical results confirm that roots of *N. tabacum* 'Xanthi-nc' are highly susceptible to an attack by *P. p. nicotianae* race 0. The extensive cell damage and cell wall disintegration observed during the infection process reflect the necrotrophic mode of nutrition of the pathogen.

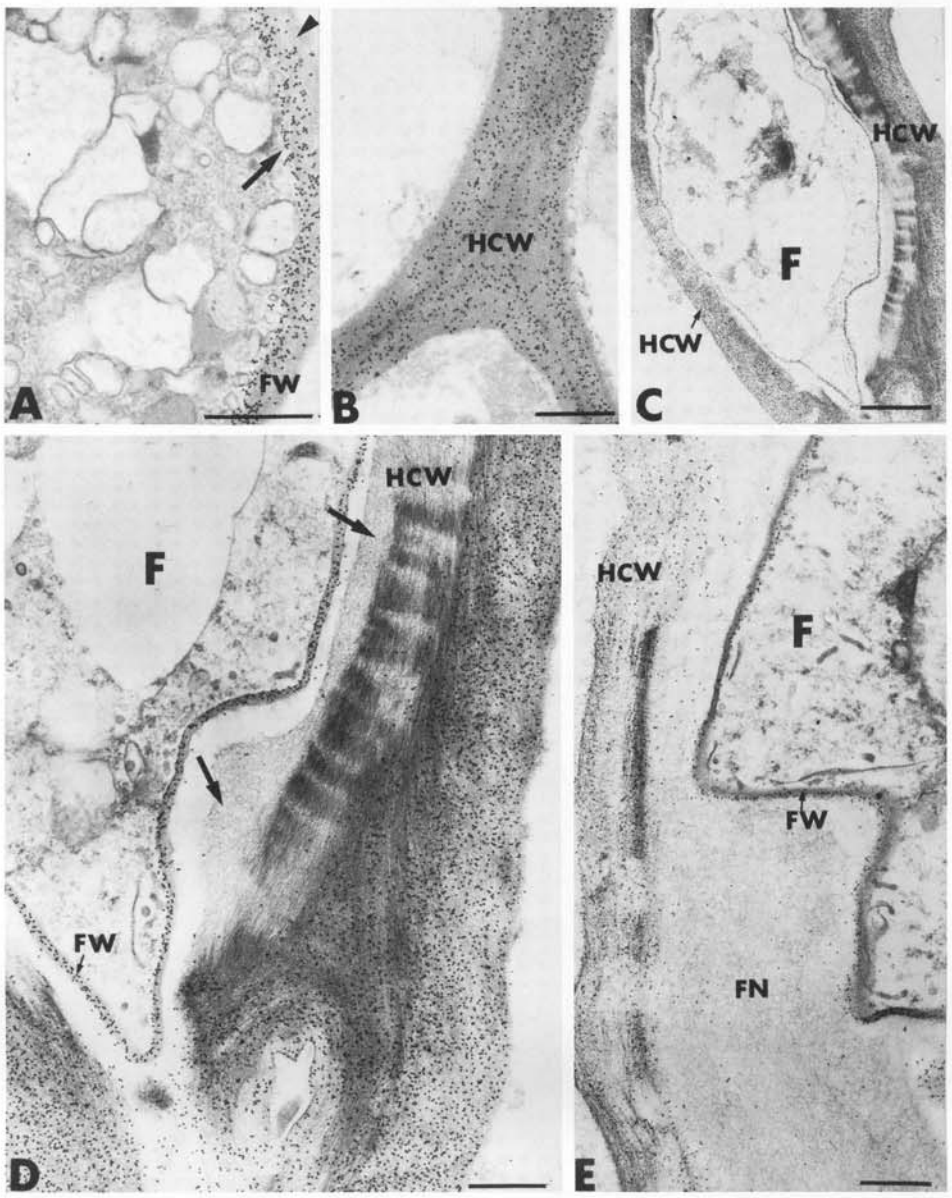

Fig. 6. Transmission electron micrographs of *Phytophthora parasitica* var. *nicotianae* infected tobacco root cells labeled with the gold-complexed exoglucanase for the localization of cellulosic β-1,4-glucans. **A,** an intense labeling occurs over the wall of a fungal cell grown in culture. Gold particles are predominantly associated with the more internal wall layers (arrow), whereas the outermost wall layers are nearly unlabeled (arrowhead) (×36,000; bar: 0.5 μm). **B,** in noninoculated tobacco roots, gold particles are evenly and abundantly distributed over host cell walls (×27,000; bar: 0.5 μm). **C,** in infected tissues, labeling occurs over the fungal cell wall and the host cell walls (×11,700; bar: 1 μm). **D,** a portion of C that shows the labeling distribution over a host cell wall adjacent to an invading hypha. Labeling is nearly abolished over the wall portion facing the fungal cell (arrows), whereas it remains intense towards the outside (×27,000; bar: 0.5 μm). **E,** the fibrillar network that accumulates in the lumen of an invaded host endodermal cell is labeled by very few gold particles (×21,600; bar: 0.5 μm). Abbreviations: FW, fungal wall; HCW, host cell wall; FN, fibrillar network.

However, the observation that the fungus is capable of triggering some defense responses during ingress into the roots corroborates the current idea that the mechanisms necessary for disease resistance are present in susceptible plants but are probably not activated with sufficient speed to halt or at least slow pathogen development (27,28).

Invasion of tobacco root tissues by hyphae of *P. p. nicotianae* resulted in significant ultrastructural changes. The epidermis and the outer cortex were the first tissues to undergo modifications within 24–48 h after inoculation, and the cortex appeared entirely colonized by the time the fungus reached the vascular parenchyma cells. Examination of the pattern of root colonization by the pathogen revealed that the fungus did not penetrate the xylem vessels even at advanced stages of infection. This by itself distinguishes *P. p. nicotianae* from other necrotrophic fungi such as *Fusarium* spp. and *Verticillium* spp., which abundantly colonize the vascular stele (14,33). However, wilting symptoms similar to those caused by vascular wilt fungi were observed on *P. p. nicotianae* infected tobacco plants. Whether these symptoms were due to the necrosis of perivascular tissues (i.e., cortex and pericycle) or were related to the occlusion of xylem vessels by large amounts of coating material remains to be determined. Why the fungus does not enter the vascular elements even through the fragile pit membrane, which is not lignified, is unknown. However, the dense deposits that were observed on the pit membranes and that occluded the pit fields in most vessels may be effective barriers to fungal penetration. In turn, these deposits also may impede lateral water transport and cause wilt. The occurrence of this material in uncolonized vessels suggests that it is not an extracellular product of hyphal growth, but rather

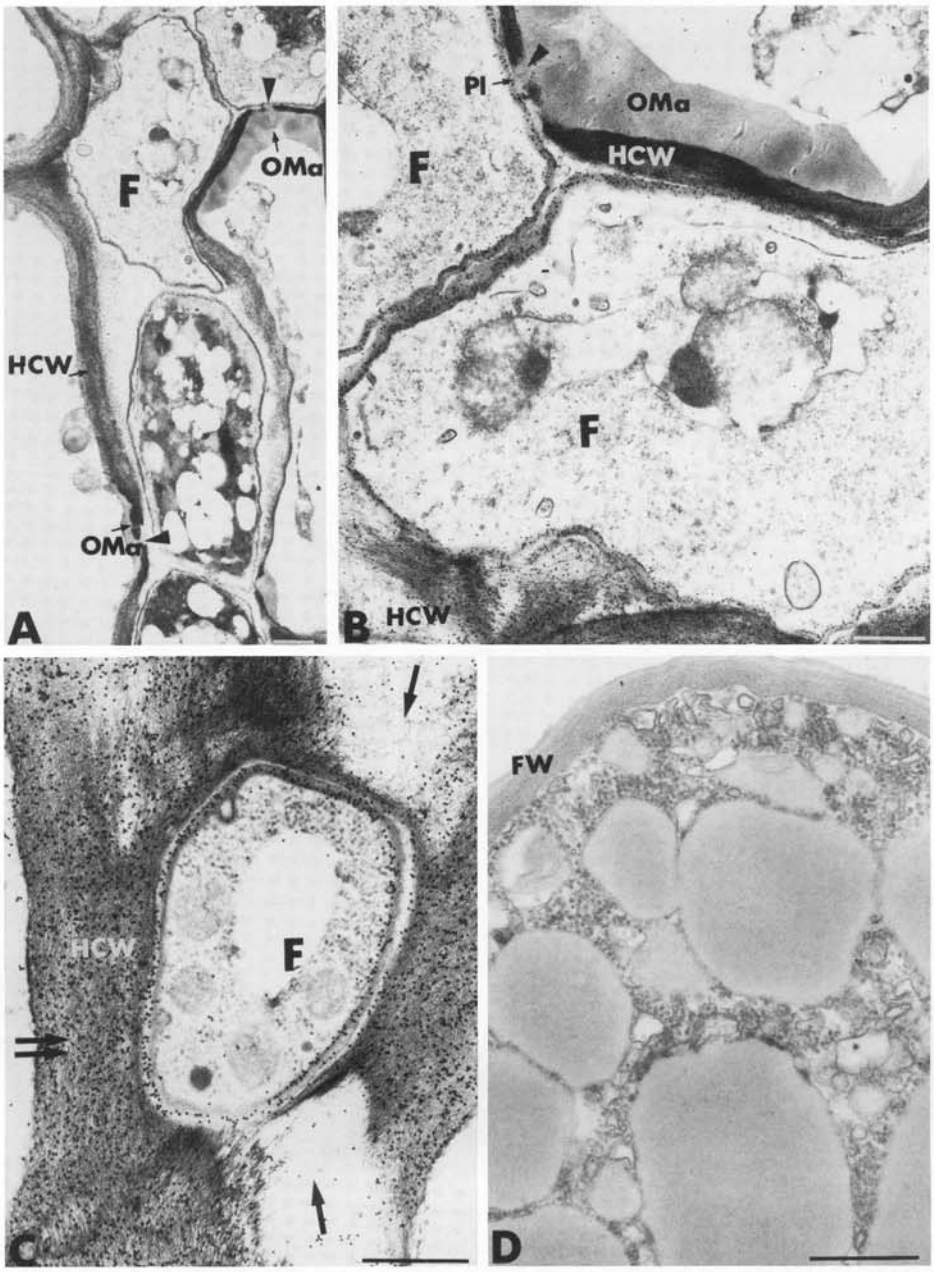

Fig. 7. Transmission electron micrographs of *Phytophthora parasitica* var. *nicotianae* infected tobacco root cells labeled with the exoglucanase-gold complex. **A,** an electron-opaque material has plugged the plasmodesma (arrowheads) between infected and uninfected host cells (×7,200; bar: 1 μm). **B,** a portion of A at a higher magnification, which shows the plugging of a plasmodesmata. Gold particles are nearly absent over the opaque material. The remaining fibrils of the altered host cell wall are labeled (×21,600; bar: 0.5 μm). **C,** a fungal cell had grown intramurally. Labeling is intense over the host cell wall (double arrows) except over highly altered areas (arrows) (×36,000; bar: 0.5 μm). **D,** control test. Previous adsorption of the exoglucanase-gold complex with β-1,4-glucans from barley resulted in an absence of labeling over the fungus cell wall (×36,000; bar: 0.5 μm). Abbreviations: F, fungus cell; OMa, opaque material; HCW, host cell wall; Pl, plasmodesma; FW, fungal wall.

occurs as a response of the plant to infection. The mechanisms that control the process of vessel wall coating is unclear, although at least two possibilities may explain this phenomenon. First, the coating material may originate from the primary cell walls of pit membranes through the swelling and stretching of preexisting polymers. This obviously would require the action of hydrolytic enzymes produced by either the fungus or the host and would require the capability of diffusing at a distance from adjacent colonized vascular parenchyma cells. However, we did not observe marked alteration of pit membranes even at the junction between xylem vessels and invaded paratracheal parenchyma cells. Second, the coating material may be deposited as new molecules synthesized in cells adjacent to xylem vessels. Whatever the origin of the coating material, this host defense response appears to be harmful for the plant itself by preventing the transfer of water and nutrients to aerial parts.

Colonization of the cortex, the endodermis, the pericycle, and the paratracheal parenchyma cells was associated with marked alterations of host cell walls and middle lamella matrices. Pathogen ingress into the roots proceeded either by intercellular growth through dissolution of middle lamellae or by direct penetration of tangential and radial primary walls. The strong alteration of middle lamella matrices without major deformation of penetrated primary cell walls supports the idea that tobacco root invasion by *P. p. nicotianae* is achieved primarily enzymatically rather than mechanically. This is consistent with the general capacity of plant pathogenic fungi, including *Phytophthora* spp. (15), to produce hydrolytic enzymes capable of degrading a number of the polymeric carbohydrates found in plant cell walls (2,24). Support for the concept of an enzymatic activity was provided by the absence of labeling over apparently altered wall areas after incubation with the gold-complexed AGL. The failure of this probe to label pectic molecules in primary wall and middle lamella areas near invading hyphae provided evidence for the release of pectic enzymes by *P. p. nicotianae*. Alteration of pectic molecules occurred in wall areas closely adjacent to fungal cells and at a distance from the point of pathogen penetration, so pectolytic enzymes may have freely diffused extracellularly and facilitated pathogen ingress through loosened middle lamella matrices and host cell walls. The extracellular diffusion of these enzymes was confirmed by the observation that pectin degradation was more pronounced in host wall layers adjacent to invading hyphae than in outermost wall layers.

Our results obtained with the exoglucanase-gold complex showed that large amounts of cellulosic β-1,4-glucans occurred in *P. p. nicotianae* cell walls. This finding confirms earlier data derived from X-ray diffraction and chemical analyses of isolated cell walls (3) and supports the current concept that oomycetes are characterized by the occurrence of cellulose in the hyphal cell walls (38). Examination of the labeling pattern obtained with the gold-complexed exoglucanase in infected tobacco root tissues revealed that *P. p. nicotianae* displayed the ability to degrade the host cell wall cellulose but to a lesser extent than that observed for pectin. The occurrence of gold particles over cell wall microfibrils that were severely altered in terms of reduced electron density and loosened structure indicated that cellulolytic enzymes were not the first enzymes to be produced by the pathogen, but were likely preceded by pectinases. Because of the ready accessibility of pectic polymers in plant cell walls, pectic molecules probably are the first polysaccharides to be degraded, followed by hemicellulosic and cellulosic polymers. The cellulosic glucans detected in *P. p. nicotianae* cell walls probably are similar to those of the host cell wall, because they were detected by the same probe. Thus, the cellulolytic enzymes excreted by the fungus possibly react with cellulosic compounds in the hyphal walls as previously shown for *Ophiostoma ulmi* in elm wood tissues (5). Surprisingly, changes in the fungal wall labeling pattern were never observed, even when the pathogen was crossing or growing within host cell walls. Whether or not this phenomenon is related to differences in the tridimensional organization of cellulose in tobacco and *P. p. nicotianae* cell walls is still unclear and deserves to be investigated further.

A large number of intercellular spaces and the lumen of several infected cells contained a network of fine intertwined fibrils that labeled specifically with the AGL-gold complex. Whether or not this unusual presence of pectic molecules corresponds to a de novo synthesis of molecules remains to be determined. A close examination of several infected root samples provided some evidence that the labeled fibrils originated from the adjacent host wall layers, the structure of which was markedly disorganized due to the probable action of fungal pectic enzymes.

Another typical feature of response to infection was the plugging of sieve pores and plasmodesmata by an amorphous, electron-opaque material. These deposits, which accumulated in phloem cells adjacent to invaded areas and at host cell-hypha contact sites, were apparently free of cellulose and pectin. However, these results must be viewed with caution, because underlying polysaccharides may be masked by the subsequent deposition of other polymers such as callose, lignin, and/or phenolic compounds (1). Accumulation of this material at specific sites such as the plasmodesmata may be a protective barrier to restrict pathogen growth and limit leakage from one cell to another, as well as to prevent the establishment of nutritional relationships between host and parasite.

In summary, the present observations demonstrate that *N. tabacum* 'Xanthi-nc', although highly susceptible to *P. p. nicotianae* infection, may develop some defense mechanisms. However, the success of a plant in restricting pathogen growth is dependent on an effective coordination of the various defense strategies and the rapidity of the overall response (8,9). Because this tobacco cultivar apparently possesses the information for resistance mechanisms to *P. p. nicotianae*, sensitization to respond more rapidly via an immunization process with a nonpathogen could be a useful method to induce resistance.

LITERATURE CITED

1. Aist, J. R. 1983. Structural responses as resistance mechanisms. Pages 33-70 in: The Dynamics of Host Defense. J. A. Bailey and B. J. Deverall, eds. Academic Press, Sydney.
2. Bateman, O. F. 1976. Plant cell wall hydrolysis by pathogens. Pages 79-103 in: Biochemical Aspects of Plant-Parasite Relationships. J. Friend and D. R. Threlfall, eds. Academic Press, New York.
3. Bartnicki-Garcia, S. 1966. Chemistry of hyphal walls of *Phytophthora*. J. Gen. Microbiol. 42:57-69.
4. Benhamou, N. 1989. Cytochemical localization of β-(1→4)-glucans in plant and fungal cells using an exoglucanase-gold complex. Electron Microsc. Rev. 2:123-138.
5. Benhamou, N., Chamberland, H., Ouellette, G. B., and Pauzé, F. J. 1987. Ultrastructural localization of β-(1→4)-glucans in two pathogenic fungi and in their host tissues by means of an exoglucanase-gold complex. Can. J. Microbiol. 33:405-417.
6. Benhamou, N., Chamberland, H., and Pauzé, F. J. 1990. Implication of pectic components in cell surface interactions between tomato root cells and *Fusarium oxysporum* f. sp. *radicis-lycopersici*. A cytochemical study by means of a lectin with polygalacturonic acid-binding affinity. Plant Physiol. 92:995-1003.
7. Benhamou, N., Gilboa-Garber, N., Trudel, J., and Asselin, A. 1988. A new lectin-gold complex for ultrastructural localization of galacturonic acids. J. Histochem. Cytochem. 36:1403-1411.
8. Benhamou, N., Grenier, J., Asselin, A., and Legrand, G. 1989. Immunogold localization of β-(1-3)-glucanases in two plants infected by vascular wilt fungi. Plant Cell 1:1209-1221.
9. Bonhoff, A., Rieth, B., Golecki, J., and Grisebach, H. 1987. Race cultivar-specific differences in callose deposition in soybean roots following infection with *Phytophthora megasperma* f. sp. *glycinea*. Planta 172:101-105.
10. Bonnet, P., Poupet, A., Abad, P., Venard, P., and Cardin, L. 1986. Induction de nécroses foliaires, de protéines B et de résistance dans les interactions tabac—*Phytophthora*. Agronomie 6:829-837.
11. Broglie, K., Chet, I., Holliday, M., Knowlton, S., Cressman, R., Biddle, P., and Broglie, R. Transgenic plants with enhanced resistance to pathogenic fungi. Science 254:1194-1197.
12. Budde, A. D., and Helgeson, J. P. 1981. Phytoalexins in tobacco callus tissue challenged by zoospores of *Phytophthora parasitica* var. *nicotianae*. (Abstr.) Phytopathology 71:206.
13. Campbell, C. L., Jacobi, W. R., Powell, M. T., and Main, C. E. 1984. Analysis of disease progression and the randomness of

occurrence of infected plants during tobacco black shank epidemics. Phytopathology 74:230-235.
14. Charest, P. M., Ouellette, G. B., and Pauzé, F. J. 1984. Cytological observations of early infection process by *Fusarium oxysporum* f. sp. *radicis-lycopersici* in tomato plants. Can. J. Bot. 62:1232-1244.
15. Clarke, D. D. 1966. Production of pectic enzymes by *Phytophthora infestans*. Nature (London) 5049:649.
16. Collins, G. B., Legg, P. D., Litton, C. C., and Kasperbauer, M. J. 1971. Inheritance of resistance to black shank in *Nicotiana tabacum* L. Can. J. Genet. Cytol. 13:422-428.
17. deZoeten, G. A., Gaard, G., Haberlach, G. T., and Helgeson, J. P. 1982. Infection of tobacco callus by *Phytophthora parasitica* var. *nicotianae*. Phytopathology 72:743-746.
18. English, J. T., and Mitchell, D. J. 1988. Relationships between the development of root systems of tobacco and infection by *Phytophthora parasitica* var. *nicotianae*. Phytopathology 78:1478-1483.
19. English, J. T., and Mitchell, D. J. 1988. Influence of an introduced composite of microorganisms on infection of tobacco by *Phytophthora parasitica* var. *nicotianae*. Phytopathology 78:1484-1490.
20. Ferrin, P. M., and Mitchell, D. J. 1986. Influence of initial density and distribution of inoculum on the epidemiology of tobacco black shank. Phytopathology 76:1153-1158.
21. Frens, G. 1973. Controlled nucleation for regulation of the particle size in monodisperse gold suspensions. Nature (London) Phys. Sci. 241:20-22.
22. Gilboa-Garber, N., Misrahi, L., and Susswein, A. J. 1984. Detection of lectins in the reproductive system and hemolymph from species of the sea hare *Aplysia*. Mar. Biol. Lett. 5:105-109.
23. Goins, R. B., and Apple, J. L. 1970. Inheritance and phenotypic expression of a dominant factor for black shank resistance from *Nicotiana plumbaginifolia* in a *Nicotiana tabacum* milieu. Tab. Sci. 14:7-11.
24. Hahn, M. G., Bucheli, P., Cervone, F., Doares, S. H., O'Neill, R. A., Darvill, A., and Albersheim, P. 1989. The roles of cell wall constituents in plant-pathogen interactions. Pages 131-181 in: Plant-Microbe Interactions. E. Nester and T. Kosuge, eds. Vol. 3. McGraw-Hill, New York.
25. Hemmes, D. E. 1983. Cytology of Phytophthora. Pages 9-40 in: Phytophtora: Its Biology, Ecology, Taxonomy, and Pathology. D. C. Erwin and S. Bartnicki-Garcia, eds. The American Phytopathological Society, St. Paul, MN.
26. Kannwisher, M. E., and Mitchell, D. J. 1978. The influence of a fungicide on the epidemiology of black shank of tobacco. Phytopathology 68:1760-1765.
27. Kuc, J. 1983. Induced systemic resistance of plants to disease caused by fungi and bacteria. Pages 191-221 in: The Dynamics of Host Defense. J. A. Bailey and B. J. Deverall, eds. Academic Press, Sidney.
28. Kuc, J. 1987. Plant immunization and its applicability of disease control. Pages 255-274 in: Innovative Approaches to Plant Disease Control. I. Chet, ed. John Wiley & Sons, New York.
29. Lamb, C. J., Lawton, M. A., Dron, M., and Dixon, R. A. 1989. Signals and transduction mechanisms for activation of plant defenses against microbial attack. Cell 56:215-224.
30. Maronek, P. M., and Hendrix, J. W. 1978. Resistance to race 0 of *Phytophthora parasitica* var. *nicotianae* in tissue cultures of a tobacco breeding line with black shank resistance derived from *Nicotiana longiflora*. Phytopathology 68:233-234.
31. McIntyre, J. L., and Dodds, J. A. 1979. Induction of localized and systemic protection against *Phytophthora parasitica* var. *nicotianae* by tobacco mosaic virus infection of tobacco hypersensitive to the virus. Physiol. Plant Pathol. 15:321-330.
32. Meins, F., and Ahl, P. 1989. Induction of chitinase and β-1,3-glucanase in tobacco plants infected with *Pseudomonas tabaci* and *Phytophthora parasitica* var. *nicotianae*. Plant Sci. 61:155-161.
33. Pegg, G. F., Gill, K., and Newsam, R. J. 1976. Transmission electron microscopy of *Verticillium albo-atrum* hyphae in xylem vessels of tomato plants. Physiol. Plant Pathol. 8:221-224.
34. Rickauer, M., Fournier, J., and Esquerré-Tugayé, M. T. 1989. Induction of proteinase inhibitors in tobacco cell suspension culture by elicitors of *Phytophthora parasitica* var. *nicotianae*. Plant Physiol. 90:1065-1070.
35. Roby, D., Broglie, K., Cressman, R., Biddle, P., Chet, I., and Broglie, R. 1990. Activation of a bean chitinase promoter in transgenic tobacco plants by phytopathogenic fungi. Plant Cell 2:999-1007.
36. Stavely, J. R. 1979. Disease resistance in *Nicotiana*: Procedures for experimental use. Pages 87-110 in: U.S. Dept. Agric., Tech. Bull. 1586. R. D. Durbin, ed.
37. Weibel, E. R. 1969. Stereological principles for morphometry in electron microscope cytology. Int. Rev. Cytol. 26:235-244.
38. Wessels, J. G. W., and Sietsma, J. H. 1981. Fungal cell walls: A survey. Pages 352-394 in: Plant Carbohydrates II. W. Tanner and F. A. Loewers, eds. Springer-Verlag, New York.